VALIDATION OF THE CFD SIMULATION OF A REDUCED SCALE STIRRED TANK WITH A THREE-BLADE HYDROFOIL IMPELLER

José C. Chambergo V., jcchambergo@pucp.edu.pe
Alex A. Pachas N., apachasn@pucp.edu.pe
Quino Valverde G., qvalver@pucp.edu.pe
Rosendo Franco R., rofranco@pucp.edu.pe
Herbert Yépez C., hyepez@pucp.edu.pe
Renato P. Gazzolo R., renato.gazzolo@pucp.edu.pe
Roberto T. Shimabukuro L., takao.shimabukuro@pucp.pe
INACOM Group, Department of Mechanical Engineering, PUCP, 1801 Universitaria Avenue, Lima-32, Perú.

Abstract: *This study reports a comparison between Computational Fluid Dynamics (CFD) simulation and experimental results on a reduced scale stirred tank with a three-blade hydrofoil impeller. The purpose is to validate CFD simulation as a procedure to understand the behavior of stirred tanks for mixing proceeses. Torque on the impeller was measured and experimental Power curve is plotted to be compared to corresponding CFD results. The Volume of Fluid (VoF) method is applied and SST k-ω model is used to simulate the fluid flow turbulence within the stirred tank. A Newtonian fluid has been considered, a fluid density of $1,623\ kg/m^3$, dynamic viscosity of $0.065\ Pa{\cdot}s$ and angular velocities between 200 and $700\ min^{-1}$. Power curves obtained show an asymptotic behavior in turbulent flow for both numerical simulation and experimental procedure. Comparison between numerical and experimental results exhibits a mean difference of 9 %. This validation demonstrates potential for general applicability on the study of industrial scale stirred tanks by means of numerical simulation.*

Keywords: *Stirred tank, Mixing process, Power Curve, hydrofoil impeller, Computational Fluid Dynamics (CFD).*

1. INTRODUCTION

Stirred tanks are common and important for various industrial applications such as: petrochemical, pharmaceutical, biotechnology, metallurgy and others (Yang and Zhou, 2015; Yapici, 2008). Moreover, a stirring process refers to force the movement by an impeller in a fluid or mixture of fluids and solid particles within a tank. In mixing process on stirred tanks, the fluid tends to move in circulatory motion but impacts on the baffles located within the tank, which results in a reduction of swirl and improved mixing efficiency (Raxón and Eddie, 2013). Fluid pressures and velocity gradients fluctuate over time within a stirred tank, generating a non-steady flow. According to Versteeg and Malalasekera (2007), such fluctuations are described in three typical scales: non - uniformities, which scale is about the diameter of the machine, periodic fluctuations associated to the pitch of the blade and small scale perturbations, associated with turbulent structures of the existing flow in any fluid machine.

Experimental techniques have been established for the development of stirred tanks, in order to establish power consumption, homogeneity of fluids, among others (Zwietering, 1958; Wu and M., 2006; Wu and Parthasarathy, 2010a; Wu and L., 2010b; Ibrahim and Baker, 2012). Moreover, relationships between variables and operating parameters can be achieved via empirical correlations from experimental tests. Some of the measures to be considered are the fluctuating velocity, the turbulence index and the rate of pumping, which are factors that assess the amount of convective flow and power demand of the stirred tank (García-Cortes and Jáuregui-Haza, 2006). However, the complexity and diversity of the pressure fluctuations and velocity gradients phenomena in an experimental analysis carries some uncertainties about the results. Therefore, good experimental results require appropriate equipment and instruments and can be expensive if not impractical.

Since the $70's$, the use of computational tools for the analysis of fluid flow and its phenomena has been increasing through improved computer technology and numerical techniques (Versteeg and Malalasekera, 2007). The Computational Fluid Dynamics (CFD) is a very useful tool to analyze turbulence phenomenon in stirred tanks (Scargiali and A., 2007). Currently, one of the most used computational tools is $\mathrm{ANSYS - CFX}^{TM}$. This tool is used for analysis and to a lesser extent for the design of fluid machines (Versteeg and Malalasekera, 2007; Shah and Lakhera, 2013).

New designs of stirred tanks in different operating scenarios can be studied through CFD techniques at a relatively low cost. These techniques can simulate and display fluid flow at steady or transient state in stirred tanks for different scales (prototype or industrial scale) and predict parameters of interest. However, it is always necessary to validate numerical simulations with experimental data (Kehn, 2013).

This paper focuses on the numerical simulation of a stirred tank with a hydrofoil impeller. The purpose is to validate numerical simulation as a procedure to understand the behavior of stirred tanks for mixing processes. Torque on the

impeller was measured and experimental Power curve is plotted to be compared to corresponding numerical results. For this purpose, different operating angular velocity values are set in the range of 200 to 700 min^{-1} and steady-state torque on the impeller shaft is determined for each one.

NOMENCLATURE

Latin

Δt	Time step		p	Pressure gradient
$\dot{m}$	Mass transfer		r	Radial distance
$\vec{v}$	Velocity of phase		Re	Reynolds number
$\vec{F}$	Force vector		S	Source term
$\vec{g}$	Gravity acceleration		S_{ij}	Mean rate-of-strain tensor
$\vec{u}$	Mixture velocity		t	Time interval
C	Clearance		U	Volume flux
D	Impeller diameter		U_a	Axial Velocity
H	Homogenized mixture height		U_f	Volume flux trough the face, based on normal velocity
H_T	Tank height			
k	Consistency index		U_{tip}	Tip Velocity
n	Index for previous time step		V	Volume of cell
$n+1$	Index for new time step		z	Axial coordinate
N_P	Power number		v	Fluid speed

Greek

α	Angle of attack		ϕ	Tank diameter
$\alpha_{q,f}$	Volume fraction		ρ	Fluid density
μ	Mixture viscosity		$\rho_{q,f}$	Density of phase
μ_t	Turbulence viscosity		σ	Surface tension

Subscripts

p	Phase p		q	Phase q

2. MATHEMATICAL MODEL

In the present study the process in the stirred tank is considered as a free surface flow biphasic transient problem. One of the phases is liquid, which represents the homogenized mixture and is modeled as a homogeneous Newtonian liquid, and the other phase is air. Mathematical model is presented from the perspective of the Volume of Fluid (*VoF*) method, which is used to describe the boundaries between the two-phase flows: liquid and air. The shear stress turbulence model SST k-ω is used, because it allows an adequate representation of turbulence effects generated by the kinetic energy transferred from the impeller to the mixture.

2.1 Volume of Fluid Method

Volume of fluid method (*VoF*) had been used for the CFD simulations to reconstruct the interface shape between the phases, homogenized mixture and air. *VoF* ensures ease of application and adequate balance between volume conservation and accuracy. *VoF* model solves the equation for the volume fraction (1) and momentum (2) in transient-state.

$$\frac{\partial(\alpha_q \rho_q)}{\partial t} + \nabla \cdot (\alpha_q \rho_q \vec{u}) = S_q + \sum_{p=1}^{n} \dot{m}_{pq} \tag{1}$$

$$\frac{\partial(\rho \vec{v})}{\partial t} + \nabla \cdot (\rho \vec{v} \vec{v}) = -\nabla p + \nabla \cdot \left[\mu \left(\nabla \vec{v} + \nabla \vec{v}^T \right) \right] + \rho \vec{g} + \vec{F} \tag{2}$$

The variable $\alpha_{q,f}$ in the volume of the stirred tank represent the volume fraction of the homogenized mixture and air, with the unity value in pure zones, and values of $0 < \alpha_{q,f} < 1$ represent the interface between both. And the phases

continuity is solved through implicit time discretization for solving the volume fraction equation. The implicit scheme requires an iterative process to solve the *VoF* equation at each time step, the implicit scheme solves the equation (3):

$$\frac{\alpha_q^{n+1}\rho_q^{n+1} - \alpha_q^n\rho_q^n}{\Delta t}\mathbf{V} + \sum_f \left(\alpha_{q,f}^{n+1}\rho_q^{n+1}U_{q,f}^{n+1}\right) = \left[S_q + \sum_p (\dot{m}_{pq} - \dot{m}_{qp})\right]\mathbf{V} \tag{3}$$

2.2 Surface tension model

The Continuum Surface Force (CSF) model is included within the *VoF* model. The CSF model incorporates the effects of the surface tension along the interface between the air and the homogenized mixture. The CSF is a non-conservative model, which converts the surface forces to volumetric forces (Brackbill and Zemach, 1992). Indeed, this model offers a source term in the momentum equation to the *VoF* implicit scheme used.

2.3 Newtonian Fluid Model

The homogenized mixture is a blend of liquid and solids, in fact, the blend has a liquid behaviour and it is similar to the water. The linear relationship between the shear stress and the rate of shear was validated with a viscometer. With the experimental results, the homogenized mixture has been modeled as an homogeneous Newtonian liquid and the main mean properties has been used for the numerical simulations. Its main mean properties are a density of $1,623\ kg/m^3$ and a dynamic viscosity of $0.065\ Pa{\cdot}s$.

2.4 SST k-ω Model

SST k-ω turbulence model is used throughout the range of operating angular velocities. This model is recommended because it allows to obtain accuracy as long as the quality mesh on the boundary layer is guaranteed. This layer is in practice extremely thin ($y^+ < 5$).
The turbulence model solves two equations, namely:

$$\frac{\partial(\rho\mathbf{k})}{\partial t} + \mathbf{div}(\rho k U) = \mathbf{div}[(\mu + \frac{\mu_t}{\sigma_\mathbf{k}})grad(\mathbf{k})] + P_\mathbf{k} - \beta^*\rho\mathbf{k}w \tag{4}$$

$$P_\mathbf{k} = (2\mu_t S_{ij} \cdot S_{ij} - \frac{2}{3}\rho k \frac{\partial U_i}{\partial x_j}\delta_{ij}) \tag{5}$$

$$\frac{\partial(\rho w)}{\partial t} + \mathbf{div}(\rho w U) = \mathbf{div}[(\mu + \frac{\mu_t}{\sigma_{w,1}})grad(w)] + \gamma_2(2\rho S_{ij} \cdot S_{ij} - \frac{2}{3}\rho w\frac{\partial U_i}{\partial x_j}\delta_{ij}) - \beta_2\rho w^2 \\ +2\frac{\rho}{\sigma_{w,2}w}\frac{\partial\mathbf{k}}{\partial x_\mathbf{k}}\frac{\partial w}{\partial x_\mathbf{k}} \tag{6}$$

For solving the equations 3 and 5, the values for the constants are: $\sigma_\mathbf{k} = 1.0$, $\sigma_{w,1} = 2.0$, $\sigma_{w,2} = 1.17$, $\gamma_2 = 0.44$, $\beta_2 = 0.083$ and $\beta^* = 0.09$.

3. MODELING PROCEDURE

The stirred tank configuration is similar as that used by the experimental results. This configuration has been modeled avoiding acute and right angles in the geometry. This consideration in the model furnishes acquire a Grid-independent solution with tetrahedral elements for the mesh. Furthermore, the boundary conditions are imposed with two important conditions: the operating angular velocity and the atmospheric pressure on the top of the stirred tank.

3.1 Geometry and Mesh

The main features of the stirred tank at reduced scale are: tank diameter $\phi = 610\ mm$, tank height is $H_T = 600\ mm$ with an homogenized mixture height $H = 480\ mm$, impeller diameter $D = 190\ mm$, clearance $C = 114\ mm$ and angle of attack of the blades $\alpha = 15°$. The geometry of the stirred tank with three-blade hydrofoil impeller must be modeled with two domains, stationary and rotatory, which allows to impose the motion of the three-blade impeller within the stirred tank. The features of the stirred tank can be seen in the Fig.1.
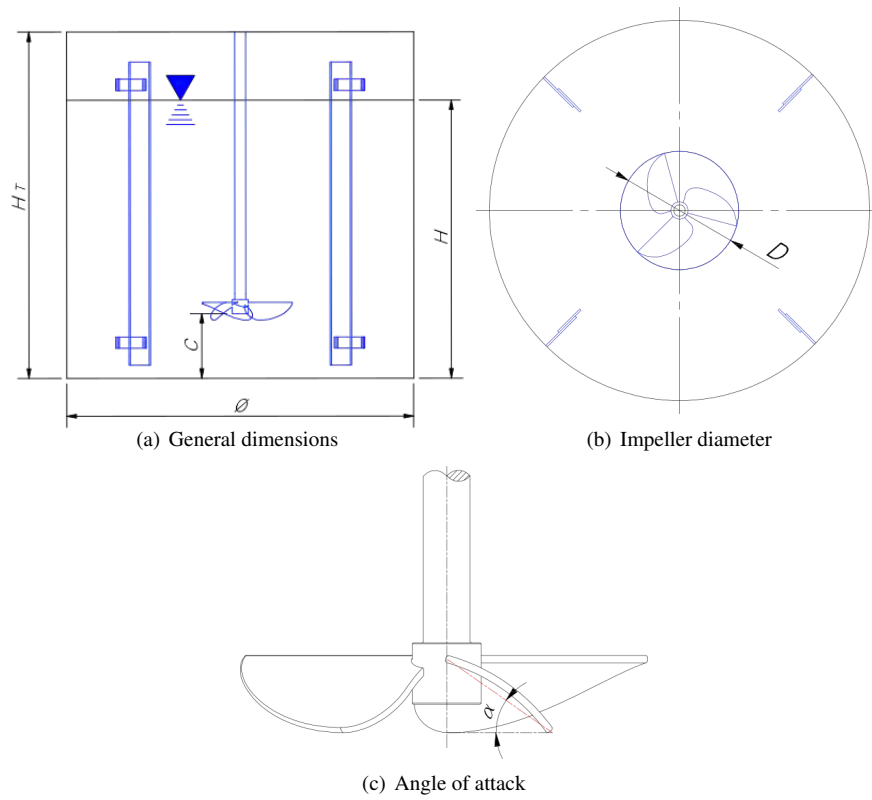
(a) General dimensions   (b) Impeller diameter

(c) Angle of attack

Fig. 1: **Schematic diagram of the scale stirred tank**

The mesh is generated for the two domains of the model, being important to consider the surfaces of coupling , three surfaces in the stationary domain and the other three in the rotatory domain. Not only, is important for the meshing the previous condition, but also it is necessary to acquire the effect of the viscosity normal to the walls of the shaft, impeller, baffles and tank. For this reason, the elements near those walls are generated as prismatic elements with 10 layers with a thickness of $1.5\ mm$. The elements close to the shaft and the three-blade hydrofoil impeller can be seen in the Fig.2. The total of elements in the stirred tank is $7'681, 205$ with a size of $10\ mm$. Grid independent results were obtained with this mesh, which has tetrahedral elements.
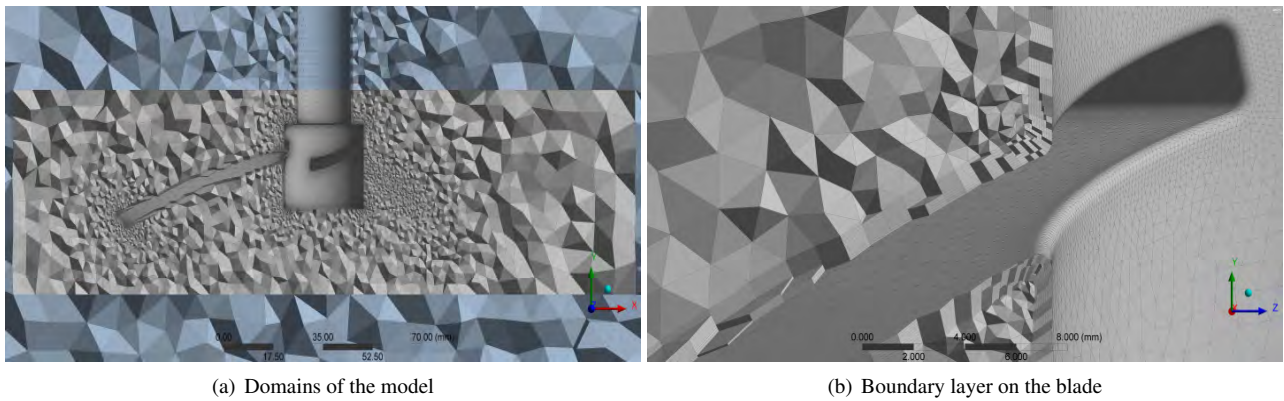

(a) Domains of the model   (b) Boundary layer on the blade

Fig. 2: **Meshing detail of the three-blade hydrofoil impeller**

3.2 Initial and Boundary contidtions

Eleven operating angular velocity values were set in the range of 200 to $700\ min^{-1}$. The upper zone of the tank is occupied by air with volume fraction of 1 and atmospheric pressure is applied on the top of the stirred tank. All the solid walls in the stirred tank were assumed with a non-slip wall boundary.

Moreover, the Slinding Mesh Modeling (SMM) is used to impose the interaction between the rotatory and stationary domain. The SMM allows to separate the two domains taking into account the transient state of the CFD simulations. The model offers a most accurate description of the flow pattern of the stirred tank, because, the flow pattern of the impeller, rotatory domain, is transferred to the stationary domain. The most important requierement for the use of the SSM is to

avoid a max cell skewness of 0.9, being the skewness value of the mesh in the stirred tank 0.74 for the CFD simulations. A transient-state problem is solved in a time interval of $t = 10\ s$ with a time step $\Delta t = 10^{-3}\ s$ The result of a steady-state problem analysis are set as initial conditions.

3.3 Numerical schemes

For the calculation of the flow field within the stirred tank has been used the *SIMPLE* algorithm. The algorithm furnishes a relationship between velocity and pressure corrections to carry out a mas conservation, then calculate the pressure field (Patankar, 1980). The solution process initializates in steady-state to ensure a better convergence and accuracy, it helps to develop adequate results of the SST k-ω model.

The Spatial discretization of the pressure is solved with the PRESTO, which uses a similar procedure to the staggered-grid scheme (Patankar, 1980). The former scheme for the interpolation of the pressure uses the discrete continuity balance for a "staggered" control volume about the face to compute the face pressure (Nichita and Thome, 2010). PRESTO scheme allows an adequate accuracy with tetrahedral mesh.

4. RESULTS

Results obtained from the CFD simulations point out a volume fraction with a suitable interface between homogenized mixture and air, and streamlines show a coherent flow pattern, both plotted in a longitudinal plane. Also, the mean y^+ ($y^+ = 2.78$) over the walls within stirred tank guarantees an adequate accuracy of the viscosity effects near the boundary layer (Versteeg and Malalasekera, 2007). Moreover, a quantitative analysis of mean axial velocity is made for three different operating angular speeds. Power curve is constructed from simulation results and is compared to corresponding experimental results.

4.1 Mean axial velocity

The profiles of the mean axial velocity at three different operating angular velocities are shown in Fig.3. The radial distance is $r = 110\ mm$, which is the third part, approximately, of the radius of the stirred tank (Fig.1 (a)). The distributions have been plotted taking into account the three representative values for the angular velocities, $200\ min^{-1}$, $450\ min^{-1}$ and $700\ min^{-1}$ and the distributions represent the axial velocity in a negative sense. The maximum values of the mean U_a/U_{tip} for $200\ min^{-1}$ is -0.0103, for $450\ min^{-1}$ is -0.0106 and for $700\ min^{-1}$ is -0.0154. It should be specified that, in regions near the interface the values for U_a/U_{tip} are from 0.0031 to 0.0058, in effect, there is an induce flow in positive sense in the three angular velocities. The Fig.3 (a) reveals a slighty velocity concentration around of the impeller domain, whereas the concentration of velocity values at $450\ min^{-1}$ (Fig.3 (b)) is better. At $700\ min^{-1}$ (Fig.3 (c)) the velocity values have increased significantly compared to the other angular velocities, even it appears some velocity values with positive sense. It could be estimated that the stirred tank has an adequate axial velocity at values close to $450\ min^{-1}$.
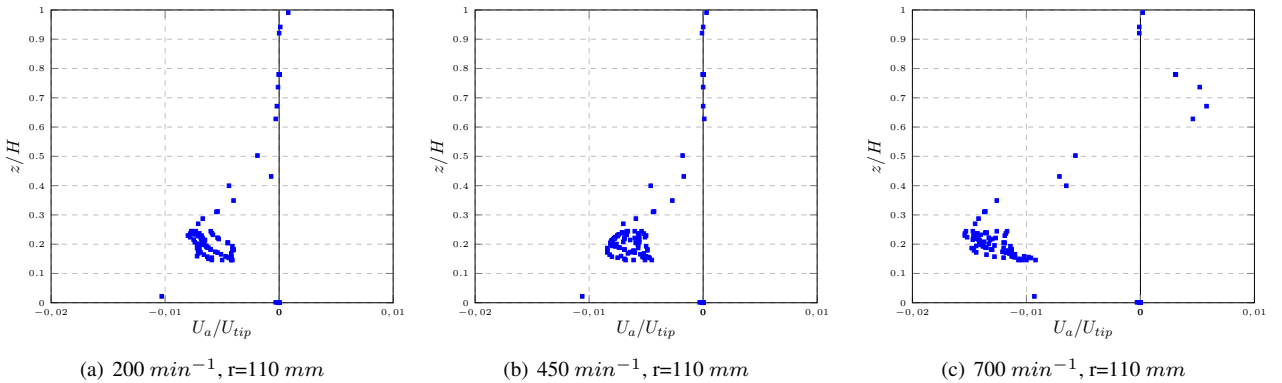

(a) $200\ min^{-1}$, r=110 mm (b) $450\ min^{-1}$, r=110 mm (c) $700\ min^{-1}$, r=110 mm

Fig. 3: **Mean axial velocity at three different angular velocites**

4.2 Liquid surface profiles and Streamlines

The free surface profile shows there is no vortex on the interface between homogenized mixture and air, Fig.4 (a); it is due to the baffles effect on the fluid flow in the stirred tank. Indeed, below of the interface, it exists only an homogenized mixture region and there is not air in this region. *VoF* allows to obtain the continuity between both phases. Streamlines have an axial tendency although the homogenized mixture has a high density and dynamic viscosity in comparison to the water, Fig.4 (b). The results of the velocity contour and the velocity vectors are showed on a transverse plane, the plane is located a distance C on the bottom of the stirred tank (see Fig.1 (a)). The contour velocity reveals, Fig.4 (c), that the highest values of velocity are in the impeller domain. Whereas, there is a slight increment of the velocity in the wall of

5

the tank, because of the baffles. Near the walls the velocity fields change when the homogenized mixture schocks with the baffles. In point of fact, the baffles allow a formation of four vortexes instead of a central vortex in close regions to the shaft and impeller. The vector velocity indicates the tendency of the vortexes formation in the stirred tank, Fig.4 (d).
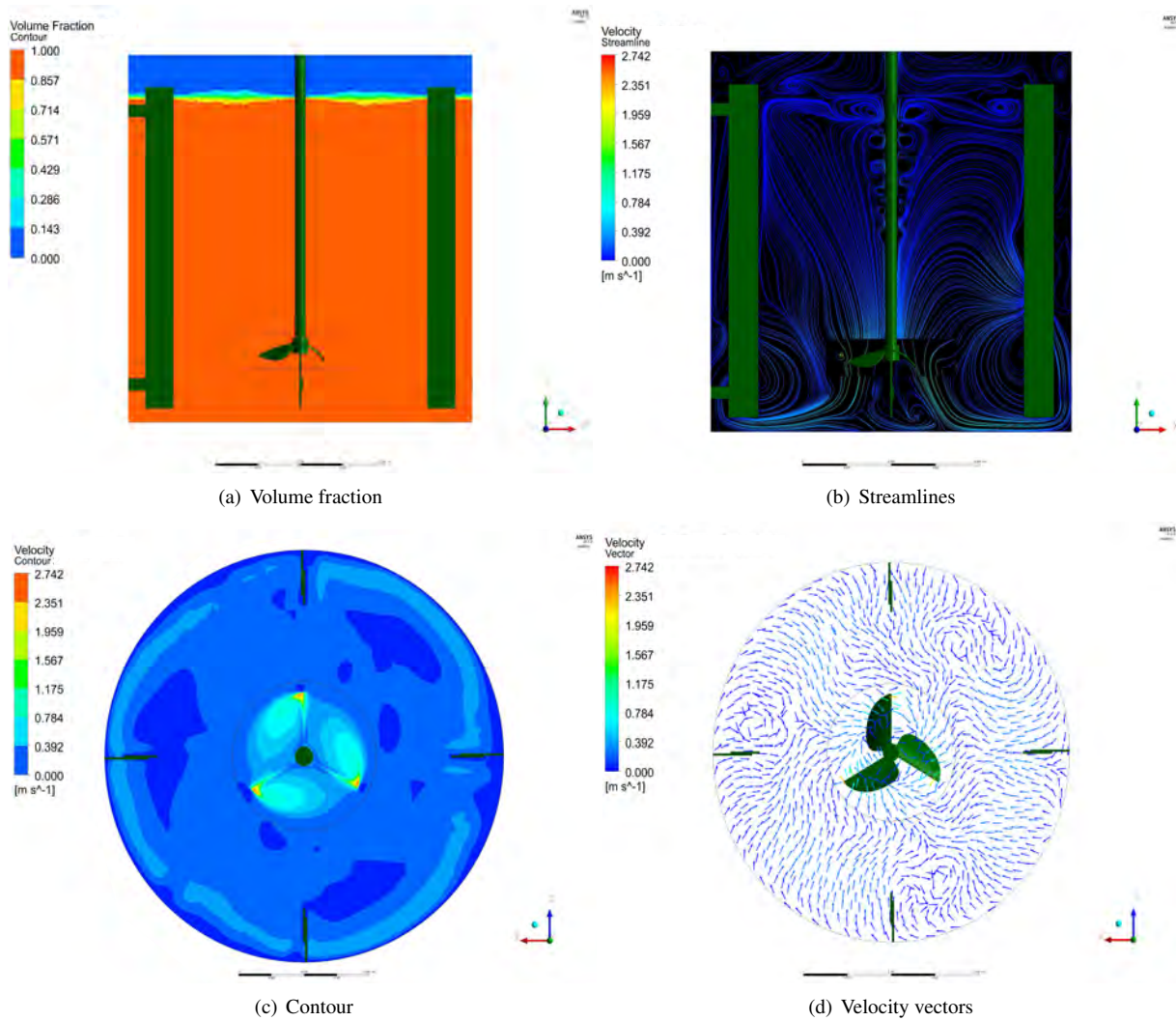

(a) Volume fraction

(b) Streamlines

(c) Contour

(d) Velocity vectors

Fig. 4: **Volume fraction and velocity distributions for 250** min^{-1}

The qualitative results have been plotted for an angular velocity of 250 min^{-1}, due to the fact that at this value the flow pattern within stirred tank has an evident axial tendency and it is according to other axial impellers. At this value could be considered an adequate flow pattern, but, it is necessary to evaluate other results, not only qualitatives but also quantitatives.

4.3 Power Curve

CFD simulations show that Power curve (Power number N_P vs. Reynolds number Re) of the hydrofoil impeller has an asymptotic behavior and it converges to 0.32, whereas experimental curve converges to 0.36 for high Reynolds number in turbulent regime; it occurs for angular velocities up to 300 min^{-1}. The comparison between numerical and experimental results exhibits a mean difference of 9 %. Indeed, both results shown in Fig.5. Numerical and experimental results are between the Power curve of the Wide and Narrow blade, which have a convergence Power number value of 0.47 and 0.23 respectively. In fact, the Power curve of the reduced scale stirred tank with a three-blade hydrofoil impeller converges to a close N_P value corresponding to a Lighting A310 impeller, which converges to 0.31 (Kresta and Atiemo-Obeng, 2016).
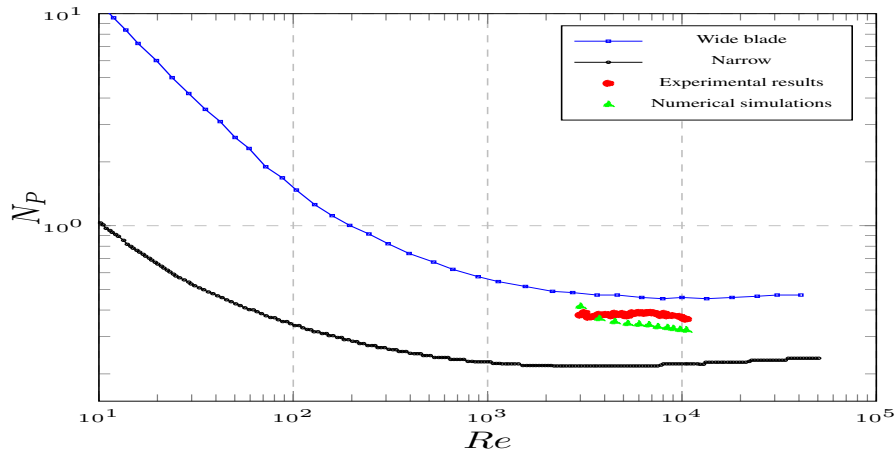
Fig. 5: **Power curve of the hydrofoil impeller**

5. CONCLUSIONS

Comparison between numerical simulations and experimental results of the stirred tank at reduced scale with three-blade hydrofoil impeller exhibits a difference of 9 %. Indeed, from CFD simulations Power number N_P converges to 0.32 while from experimental results N_P converges to 0.36 for high Reynolds number, it occurs for angular velocities up to 300 min^{-1}. These results demonstrate a good accuracy of the CFD procedure, in fact the Power curve of this three-blade hydrofoil impeller converges to a N_P value corresponding to a Lighting A310 impeller. Streamlines and mean axial velocity distributions show the axial tendency of the flow patterns generated by the three-blade hydrofoil impeller, which is the main physical characteristic of this kind of stirred tanks with hydrofoil impellers.

6. ACKNOWLEDGEMENTS

7. REFERENCES

Brackbill, J. U., K.D.B. and Zemach, C., 1992. "A continuum method for modeling surface tension". *Journal of Computational Physics*, Vol. 100, pp. 335–354.

García-Cortes, D. and Jáuregui-Haza, U., 2006. "Hidrodinámica en tanques agitados con turbina de disco con paletas planas". *Universidad de Antioquia – Colombia, Revista Facultad de Ingeniería*, Vol. 38, pp. 97–113.

Ibrahim, S., J.S.W.D. and Baker, I., 2012. "Zwieterings equation for the suspension of porous particles and the use of curved blade impellers". *International Journal of Chemical Engineering*, Vol. 2012, p. 13.

Kehn, R.O., 2013. "How computational fluid dynamics is applied to mixer design". *International Journal of Chemical Engineering*.

Kresta, S., E.A.D.D. and Atiemo-Obeng, V., 2016. *Advances in Industrial Mixing*. Wiley, USA.

Nichita, B., Z. and Thome, J.R., 2010. "A vof method coupled with a dynamic contact angle model for simulation of two-phase flows with partial wetting". *7th International Conference on Multiphase Flow*.

Patankar, S.V., 1980. *Numerical Heat Transfer and Fluid Flow*. Hemisphere Publishing Corporation, USA.

Raxón, D. and Eddie, H., 2013. "Diseño de un sistema de mezclado para la producción de suavizantes en la industria textil". *Tesis de Grado, Facultad de Ingeniería, Universidad San Carlos de Guatemala*.

Scargiali, F., D.A.G.F. and A., B., 2007. "Diseño de un sistema de mezclado para la producción de suavizantes en la industria textil". *Chemical EngineeringResearch and Design*, Vol. 85, pp. 637–646.

Shah, S. R., J.S.V.P.R.N. and Lakhera, V.J., 2013. "Cfd for centrifugal pumps: a review of the state of the art, procedia engineering". *Chemical EngineeringResearch and Design*, Vol. 51, pp. 715–720.

Versteeg, H.K. and Malalasekera, W., 2007. *An Introduction to Computational Fluid Dynamics: The Finite Volume Method*. Pearson Education, England.

Wu, J., G.L.N.B. and M., N., 2006. "Energy efficiency study on axial flow impellers". *Chemical Engineering and Processing*, Vol. 45, pp. 625–632.

Wu, J., G.L.W.S. and Parthasarathy, R., 2010a. "Energy efficiency slurry holding and transport, minerals engineering". Vol. 23, pp. 705–712.

Wu, J., N.B. and L., G., 2010b. "Energy efficiency high solids loading agitation for the mineral industry". *Canadian Journal of Chemical Engineering*, Vol. 88, pp. 287–294.

Yang, F.L. and Zhou, S.J., 2015. "Free surface turbulent flow in an unbaffled stirred tank: Detached eddy simualtion and vof study". *Chemical and Biochemical Engineering Quartly*, Vol. 29, pp. 395–403.

Yapici, K., 2008. "Numerical investigation of the effect of the rushton type turbine design factors on agitated tank flow characteristics". *Chemical Engineering and Processing: Process Intensification*, Vol. 47, pp. 1340–1349.

Zwietering, T.N., 1958. "Suspension of solids in liquid by agitators". *Chemical Engineering Science*, Vol. 8, pp. 244–253.

8. RESPONSIBILITY NOTICE

The authors of this research: **José Chambergo**, **Alex Pachas**, **Quino Valverde**, **Rosendo Franco**, **Herbert Yépez**, **Renato Gazzolo** and **Roberto Shimabukuro** are the solely responsible for the printed material included in this paper.